

Configurational Entropy and Adam-Gibbs Relation for Quantum Liquids

Yang Zhou^{1,2}, Ali Eltareb^{1,2}, Gustavo E. Lopez^{3,4},
Nicolas Giovambattista^{1,2,3}

¹Ph.D. Program in Physics, The Graduate Center of the City
University of New York, New York, 10016, NY, United States.

²Department of Physics, Brooklyn College of the City University of
New York, New York, 11210, NY, United States.

³Ph.D. Program in Chemistry, The Graduate Center of the City
University of New York, New York, 10016, NY, United States.

⁴Department of Chemistry, Lehman College of the City University of
New York, New York, 10468, NY, United States.

Contributing authors: yzhou4@gradcenter.cuny.edu;
aeltareb@gradcenter.cuny.edu; gustavo.lopez1@lehman.cuny.edu;
ngiovambattista@brooklyn.cuny.edu;

Abstract

As a liquid approaches the glass state, its dynamics slows down rapidly, by a few orders of magnitude in a very small temperature range. In the case of light elements and small molecules containing hydrogen (e.g., water), such a process can be affected by nuclear quantum effects (due to quantum fluctuations/atoms delocalization). In this work, we apply the potential energy landscape (PEL) formalism and path-integral computer simulations to study the low-temperature behavior of a Lennard-Jones binary mixture (LJBM) that obeys *quantum* mechanics. We show that, as for the case of classical liquids, (i) a configurational entropy S_{IS} can be defined, and (ii) the Adam-Gibbs equation, which relates the diffusion coefficient of a liquid and its S_{IS} , holds for the studied *quantum* LJBM. Overall, our work shows that one theoretical approach, the PEL formalism, can be used to describe low-temperature liquids close to their glass transition, independently of whether the system obeys classical or quantum mechanics.

1 Introduction

Glasses, or amorphous solids, are out-of-equilibrium systems that can be formed by different routes, including cooling a liquid sufficiently fast so crystallization can be avoided [1–4]. The behavior of liquids close to the glass state, and during the associated liquid-to-glass transition have been the focus of numerous studies over the last few decades [5–8], and various theoretical approaches have been proposed to describe these systems [2, 9–12]. In most theoretical/computational studies, the liquids/glasses are treated classically which is justified given that many common glass-formers, such as silica, are composed of heavy atoms and exhibit a high glass transition temperature (> 1000 K). There are, however, liquids that vitrify at relatively low temperatures where nuclear quantum effects (due to the atoms delocalization) can play a relevant role. This is the case of small molecules that contain hydrogen, such as water [13], where isotope substitution effects are non-negligible even close to room temperature [14, 15]. Obviously, nuclear quantum effects (NQE) play a relevant role in light-element liquids, such as H_2 and He (even at temperatures where classical statistics holds [16–18]). We also note that there are quantum systems, other than liquids, that exhibit a glass transition. These include electrons in metals [19, 20] and spin systems [21–23]. It remains unclear how quantum mechanics may change the behavior of low-temperature liquids close to their glass transition temperature, relative to the classical case. For example, an extension of mode coupling theory suggest that including quantum effects may increase the glass transition temperature of a liquid [24]. In other systems, quantum effects may erase the glass state altogether [25].

A well-established theoretical framework to study *classical* low-temperature liquids and glasses is the potential energy landscape (PEL) formalism [26, 27]. The PEL formalism is based on statistical mechanics [28–30] and has been applied extensively to describe the behavior of atomistic [31–33] and molecular liquids [34, 35]. The PEL formalism provides (i) a qualitative description of classical liquids/glasses, and (ii) under simple approximations, it also provides the Helmholtz free energy and equation of state of the system [35–40]. In previous studies [13, 41, 42], we extended the PEL formalism to the case of liquids that obey quantum mechanics. It was shown that (i') the same qualitative description of classical liquids and glasses, based on the PEL formalism, can be extended to quantum liquids. Moreover, path-integral molecular dynamics of water suggest that (ii') the PEL formalism may be used to predict the thermodynamic properties of liquids at low temperature in the presence of NQE [13].

In this work, we build upon the work presented in Refs. [13, 41, 42] and extend the definition of configurational entropy to the case of quantum liquids. The configurational entropy S_{IS} [26–28], as well as the associated Kauzmann temperature [5], play important roles in the description of liquids and glasses in general [2, 28, 43–45], and are essential to predict the thermodynamic behavior of low-temperature liquids, including the corresponding equation of state. To do so, in this work, we hypothesize that the distribution of local minima (inherent structures, IS) in the PEL of the *quantum* liquid is identical to the distribution of IS in the PEL of the corresponding *classical* liquid counterpart. This hypothesis, based on path-integral computer simulations of various model liquids, establishes a direct link between the configurational

entropies of the quantum and associated classical liquid. Using ring-polymer molecular dynamics (RPMD) simulations of a model liquid, we test that the configurational entropy defined in this study is consistent with relationships required by the PEL formalism.

It has been found that, for many classical liquids, the configurational entropy controls the corresponding liquid’s dynamics. Specifically, classical molecular dynamics (MD) simulations of different liquids, including Lennard-Jones binary mixtures (LJBM) [31], silica [32], and water [46, 47], show that the diffusion coefficient of the atoms/molecules in the system depends on the configurational entropy as predicted by the Adam-Gibbs (AG) relation [6, 40, 47]. This implies that, at a given temperature, not only the thermodynamics but also the dynamics of the liquids are controlled by the PEL topography. In this study, we also perform ring-polymer MD (RPMD) simulations and show that the AG relation, with the configurational entropy introduced here, holds for the model quantum liquid studied.

2 Methods

In this work, we perform classical MD and RPMD simulations of the LJBM system defined in Ref. [48]. The LJBM model liquid is a good glass-former that has been studied extensively in the past using classical MD simulations [43, 49, 50]. We consider a LJBM composed of $N_A = 800$ type-A and $N_B = 200$ type-B particles interacting via Lennard-Jones pair interaction potentials $V_{\alpha\beta}(r) = 4\epsilon_{\alpha,\beta}[(\sigma_{\alpha\beta}/r)^{12} - (\sigma_{\alpha\beta}/r)^6]$ with $\alpha\beta \in \{A, B\}$. Following Ref. [48], we use reduced units where $\sigma_{AA} = 1.0, \sigma_{BB} = 0.80, \sigma_{AB} = 0.88$ (length), $\epsilon_{AA} = 1.0, \epsilon_{BB} = 0.5, \epsilon_{AB} = 1.5$ (energy), and $m_A = m_B = 1.0$ (mass); LJ pair interactions are truncated and shifted at a cutoff distance $r_{c,\alpha\beta} = 2.5 \sigma_{\alpha\beta}$, as implemented in the original work of Kob and Andersen [48]. Moreover, we also add a switching function to the pair interaction potentials, as implemented in OpenMM [51], to make the forces smooth functions of the inter-particle distance r . The switching function only affects the LJ pair interaction potential at inter-particle distances $r_{s,\alpha\beta} < r < r_{c,\alpha\beta}$ where $r_{s,\alpha\beta} = 0.9 r_{c,\alpha\beta}$. The system is cubic and periodic boundary conditions apply in all three directions.

As for the case of path-integral molecular dynamics (PIMD) simulations, the RPMD technique is based on the path integral formulation of statistical mechanics (see below) and they can be used to calculate thermodynamic (e.g., pressure) and structural properties (e.g., radial distribution functions) of a liquid in the presence of NQE. In PIMD/RPMD simulations, each atom of the system is represented by a ring-polymer composed of n_b beads; by setting $n_b = 1$, the PIMD/RPMD simulation technique reduces to classical MD simulations. To obtain $D(T)$, we use the RPMD technique which is based on RPMD simulations. As explained in Refs. [52, 53], from the RPMD trajectory, one can calculate, approximately, the dynamical properties of the quantum system. In this work, $D(T)$ is calculated from the long-term behavior of the mean-square displacement of the ring-polymer centroids obtained from the RPMD simulations at constant temperature (see, e.g., [13, 54, 55]).

To understand the differences in the PEL properties of the quantum and classical LJBM, we follow Refs. [41, 42] and study a family of LJBMs each characterized by a

different value of the Planck's constant h . The quantum character of a liquid increases with increasing values of h since the atom delocalization becomes more pronounced as h increases (see below). In this study, we consider the cases $h_0 = 0.0000$, $h_a = 0.2474$, $h_b = 0.5000$, and $h_c = 0.7948$ (in reduced units of $\sigma_{AA}(\epsilon_{AA}m)^{1/2}$). The case $h = h_0$ corresponds to the classical liquid where the ring-polymers are collapsed at all times (for $h = 0$, the spring constant of the ring-polymers is $k^{sp} \rightarrow \infty$; see below). Hence, for the case $h = h_0$, we perform classical MD simulations. We note that the values of $h = h_a, h_b, h_c$ considered here are not negligible; for example, as discussed in detail in Ref. [42] one obtains $h = 1.78$ and $h \approx 0.18$ (in reduced units) for the case of H_2 and argon, respectively.

Most of the RPMD simulations are performed with $n_b = 10$ beads per ring-polymer. However, to test for n_b -effects, we also run RPMD simulations using $n_b = 20, 40$ ($h = h_c$). Classical MD simulations are run by setting $n_b = 1$ in the RPMD simulations. All computer simulations are performed at constant (N, V, T) for the density $\rho = 1.2$ ($V/N = 9.4, N = 1000$) and extend over a wide range of temperatures. Additional computer simulations at constant (N, V, T) are performed at $T = 5.0$ and over a wide range of volumes to calculate the total entropy of the system. The temperature is controlled by using a local PILE thermostat with stochastic collision frequency $\gamma = 0.6$. At a given state point, the starting configuration of the RPMD simulation is taken from an independent equilibrium simulation performed at a very high temperature, $T = 5.0$. Equilibrium RPMD simulations extend for $t_{eq} \geq 100 \tau_\alpha$ where τ_α is the relaxation time of the system defined as the time at which the mean-square displacement (MSD) of the type-A particles is $1.0 \sigma_{AA}^2$. To obtain a large number of IS, we perform very long production runs, of $t \geq 1000 \tau_\alpha$ (see below). All the RPMD simulations are performed using the OpenMM (version 7.3.0) software package [51] modified to include the target Planck's constant h . In the OpenMM computer simulations, the atoms mass is set to $m_A = 39.948 \text{ amu}$, $\sigma_{AA} = 1.0 \text{ \AA}$, and $\epsilon_{AA} = 1.0 \text{ kJ/mol}$ (but all quantities are reported in reduced units). The simulation time step for MD/RPMD is $dt = 0.01 \text{ ps}$ ($T \leq 1.0$) and $dt = 0.001 \text{ ps}$ ($T \in (1.0, 5.0]$) for h_0, h_a, h_b , and $dt = 0.005 \text{ ps}$ ($T \leq 1.0$) and $dt = 0.0005 \text{ ps}$ ($T \in (1.0, 5.0]$) for $h = h_c$.

From the long RPMD production runs, at a given temperature, we extract more than 1000 independent configurations. Two configurations are considered to be independent if they are separated in time by, at least, $\delta t = \tau_\alpha$. For each of these configurations, we calculate the corresponding IS by minimizing the potential energy of the system using the L-BFGS-B algorithm (the potential energy minimization is performed using the *scipy.optimize* routine in Python [56] with an error tolerance of 10^{-12} , with the forces and total potential energy obtained from the OpenMM software package using the OpenCL platform with double precision). The IS energy is obtained directly from the minimization algorithm. For each IS, we also calculate analytically the components of the mass-weighted Hessian matrix. The mass-weighted Hessian matrix is then diagonalized to calculate the corresponding eigenvalues which provide the normal mode vibrational frequencies of the system (diagonalization is performed using the *Numpy* linear algebra package in Python [57]).

3 The Potential Energy Landscape Formalism for Quantum Liquids

The PEL formalism provides a compact expression for the canonical partition function of the classical/quantum system of interest, $Q(N, V, T)$. Next, we present a brief overview of the PEL formalism for a *quantum* liquid composed of N atoms (not necessarily identical); the generalization to molecular liquids is straightforward (see, e.g., Ref. [13]).

Defining a PEL for a quantum liquid. For a quantum system, the canonical partition function is given by

$$Q(N, V, T) = \text{Tr}(\hat{\rho}) \quad (1)$$

where $\text{Tr}(\hat{\rho})$ is the trace of the density operator $\hat{\rho} = \exp(-\beta\hat{H})$ and \hat{H} is the Hamiltonian operator of the system,

$$\hat{H} = \sum_{i=1}^N \frac{\hat{\mathbf{p}}_i^2}{2m_i} + U(\hat{\mathbf{r}}_1, \hat{\mathbf{r}}_2, \dots, \hat{\mathbf{r}}_N) \quad (2)$$

In Eq. 2, $U(\hat{\mathbf{r}}_1, \hat{\mathbf{r}}_2, \dots, \hat{\mathbf{r}}_N)$ is the potential energy operator, and $(\hat{\mathbf{r}}_i, \hat{\mathbf{p}}_i)$ are the position and momentum operators associated with atom $i = 1, 2, \dots, N$ ($\beta = 1/k_B T$ where k_B is the Boltzmann's constant).

Using the path-integral formulation of quantum statistical mechanics, it can be shown that the canonical partition function of the quantum liquid (Eq. 1) is *identical* to the canonical partition function of a *classical* system of N (distinguishable) ring-polymers composed of $n_b \rightarrow \infty$ (distinguishable) beads [58, 59]. Specifically,

$$Q(N, V, T) = \lim_{n_b \rightarrow \infty} \frac{1}{h^{3n_b N}} \int_V \left(\prod_{i=1}^N d\mathbf{r}_i^1 \cdots d\mathbf{r}_i^{n_b} \right) \int_{-\infty}^{\infty} \left(\prod_{i=1}^N d\mathbf{p}_i^1 \cdots d\mathbf{p}_i^{n_b} \right) \exp(-\beta \mathcal{H}_{RP}(\mathbf{P}, \mathbf{R})) \quad (3)$$

where

$$\mathcal{H}_{RP}(\mathbf{P}, \mathbf{R}) = \sum_{i=1}^N \sum_{k=1}^{n_b} \frac{(\mathbf{p}_i^k)^2}{2m'_i} + \sum_{i=1}^N \sum_{k=1}^{n_b} \frac{1}{2} k_i^{sp} (\mathbf{r}_i^{k+1} - \mathbf{r}_i^k)^2 + \frac{1}{n_b} \sum_{k=1}^{n_b} U(\mathbf{r}_1^k, \mathbf{r}_2^k, \dots, \mathbf{r}_N^k) \quad (4)$$

is the Hamiltonian of the classical ring-polymer system. For each atom $i = 1, 2, \dots, N$ of the quantum liquid with mass m_i , there is one and only one ring-polymer i in the ring-polymer system associated to it. The spring constant of the corresponding ring-polymer is given by $k_i^{sp} = \frac{m_i n_b}{(\hbar\beta)^2}$ and the mass of the corresponding beads are given by $m'_i = n_b m_i$. In Eq. 3, $(\mathbf{r}_i^k, \mathbf{p}_i^k)$ are the vector position and momentum of the k -th bead of the i -th ring-polymer ($\mathbf{R} = \{\mathbf{r}_i^k\}$ and $\mathbf{P} = \{\mathbf{p}_i^k\}$; $i = 1, 2, \dots, N$, $k = 1, 2, \dots, n_b$). In Eq. 4, and throughout this work, $\mathbf{r}_i^1 = \mathbf{r}_i^{n_b+1}$ for $i = 1, 2, \dots, N$ since the polymers are ring-polymers.

Eq. 4 implies that the potential energy of the ring-polymer system is given by

$$\mathcal{U}_{RP}(\mathbf{R}) = \sum_{i=1}^N \sum_{k=1}^{n_b} \frac{1}{2} k_i^{sp} (\mathbf{r}_i^{k+1} - \mathbf{r}_i^k)^2 + \frac{1}{n_b} \sum_{k=1}^{n_b} U(\mathbf{r}_1^k, \mathbf{r}_2^k, \dots, \mathbf{r}_N^k). \quad (5)$$

As explained in Ref. [41, 42], the function $\mathcal{U}_{RP}(\mathbf{R})$ defines a PEL that can be associated to the given quantum liquid. By applying the PEL formalism (originally proposed to study classical liquids [26]) to the PEL defined by Eq. 5, one can study the behavior of quantum liquids and, in particular, extract the corresponding thermodynamic properties [13, 42]. We note that, strictly speaking, the above expressions hold for $n_b \rightarrow \infty$. However, in path-integral computational studies, one chooses a sufficiently large value of n_b for which the thermodynamic properties of the system of interest converge (i.e., they no longer vary upon further increase in n_b).

The PEL formalism provides a simple understanding for the behavior of low-temperature liquids and glasses. Specifically, within the PEL formalism, a classical/quantum liquid is represented by a point on the PEL that moves over time (in the case of the quantum liquid, such a PEL is given by Eq. 5 with a fix value of n_b). At high temperatures, the liquid has sufficient kinetic energy to overcome the potential energy barriers of the PEL and hence, it can explore different basins of the PEL. In the liquid state, the molecules/atoms are able to diffuse with time and the system moves on the PEL describing a trajectory. Instead, in the glass state, the molecules/atoms of the system are only able to vibrate about fix positions. Accordingly, the representative point of the system in the PEL is limited to move within a single basin, about the corresponding local minimum or inherent structure (IS). While this picture holds for classical liquids and quantum liquids/ring-polymer systems, important differences exist in the corresponding PEL formalism. Among them is the fact that the PEL of a quantum liquid is T -dependent (since the spring constant $k_i^{sp} \propto T^2$) while the PEL of a classical system is not.

Partition function in the PEL formalism. As explained in detail in Refs. [13, 42], in the PEL formalism, the partition function of a quantum liquid (Eqs. 1 and 3) can be written as,

$$Q(N, V, T) = \sum_{e_{IS}} e^{-\beta(e_{IS} - T S_{IS}(N, V, T, e_{IS}) + F_{vib}(N, V, T, e_{IS}))} \quad (6)$$

where $S_{IS}(N, V, T, e_{IS})$ is the configurational entropy of the system and $F_{vib}(N, V, T, e_{IS})$ is the vibrational Helmholtz free energy of the system. Both quantities are precisely defined in the PEL formalism; see Refs. [13, 42]. $S_{IS}(N, V, T, e_{IS})$ quantifies the number of IS available in the PEL with a given energy e_{IS} . $F_{vib}(N, V, T, e_{IS})$ is the contribution to the Helmholtz free energy of the system, $F(N, V, T)$, due to the explorations (by the system) of the PEL basins with IS energy e_{IS} .

The sum in Eq. 6 runs over all IS energies e_{IS} available in the PEL. In the thermodynamic limit, one may employ the saddle point approximation, so that only the term that maximizes the sum in Eq. 6 dominates. i.e.,

$$Q(N, V, T) \approx e^{-\beta(E_{IS} - TS_{IS}(N, V, T, E_{IS}) + F_{vib}(N, V, T, E_{IS}))} \quad (7)$$

where $E_{IS}(N, V, T)$ is the solution to the following equation,

$$1 - T \left(\frac{\partial S_{IS}(N, V, T, e_{IS})}{\partial e_{IS}} \right)_{N, V, T} + \left(\frac{\partial F_{vib}(N, V, T, e_{IS})}{\partial e_{IS}} \right)_{N, V, T} = 0 \quad (8)$$

In computational studies, one identifies $E_{IS}(N, V, T)$ with the average value of e_{IS} sampled by the system at the given working conditions (N, V, T) .

3.1 Gaussian and Harmonic PEL

A common approximation in PEL studies is to assume that the PEL is Gaussian [27, 28, 43], i.e., that the distribution of IS with energy e_{IS} available in the PEL is given by a Gaussian distribution

$$\Omega_{IS}(N, V, T, e_{IS}) \approx \frac{1}{\sqrt{2\pi}\sigma} e^{\alpha N} e^{-(e_{IS} - E_0)^2 / 2\sigma^2} \quad (9)$$

This implies that the configurational entropy of the system is given by

$$S_{IS}(N, V, T, e_{IS}) \approx k_B \left[\alpha N - \frac{(e_{IS} - E_0)^2}{2\sigma^2} \right] \quad (10)$$

Here, α , E_0 , and σ are PEL variables that depend on (V, T) . Importantly, MD/PIMD simulations of very different liquids, including LJBM [31, 60], water [13, 39, 46], ortho-terphenyl [37], and water-like monatomic systems [42, 61], indicate that the corresponding PEL is Gaussian.

Another common approximation in the PEL formalism is to assume that the PEL basins are quadratic functions (of the atoms/ring-polymer beads coordinates) near the corresponding IS. Under the harmonic approximation of the PEL, one can show that

$$F_{vib}(N, V, T, e_{IS}) \approx F_{vib}^{harm}(N, V, T, e_{IS}) = 3Nn_b k_B T \ln(\beta \hbar \omega_0) + k_B T \mathcal{S}(N, V, T, e_{IS}) \quad (11)$$

where

$$\mathcal{S}(N, V, T, e_{IS}) \approx \left\langle \ln \left(\prod_{j=1}^{3n_b N} (\omega_j / \omega_0) \right) \right\rangle_{e_{IS}} \quad (12)$$

is the basin-shape function. The $3n_b N$ values $\{\omega_j^2 = \omega_j^2(N, V, T, e_{IS})\}$ are the eigenvalues of the *mass-weighted* Hessian matrix of the ring-polymer system evaluated at the IS with energy e_{IS} ; $\langle \dots \rangle_{e_{IS}}$ indicates an average over all basins of the PEL with

energy e_{IS} . The constant ω_0 is an arbitrary quantity that makes the argument of $\ln(\dots)$ dimensionless. $\mathcal{S}(N, V, T, e_{IS})$ quantifies the average local curvature of the PEL basins with IS energy e_{IS} and it is the only term in Eq. 11 that makes F_{vib} dependent on the PEL of the system. We note that Eqs. 7-12 also apply to the case of classical liquids. However, since the PEL of classical liquids is T -independent, the topographic properties of the PEL are also T -independent; specifically, $S_{IS} = S_{IS}(N, V, e_{IS})$, $\omega_j = \omega_j(N, V, e_{IS})$ and $\mathcal{S} = \mathcal{S}(N, V, e_{IS})$.

In the PEL formalism, the Helmholtz free energy of the system, $F(N, V, T) = -k_B T \ln(Q(N, V, T))$, follows directly from Eq. 7,

$$F(N, V, T) = E_{IS}(N, V, T) - TS_{IS}(N, V, T, E_{IS}) + F_{vib}(N, V, T, E_{IS}) \quad (13)$$

In the case of a Gaussian and Harmonic approximation of the PEL (Eqs. 10 and 11), it can be shown from Eq. 13 that the free energy of the quantum liquid can be expressed in terms of only three PEL variables $\{\alpha, E_0, \sigma\}$, and the eigenvalues of the mass-weighted Hessian matrix of the corresponding ring-polymer system; see, e.g., Refs. [27–29, 42]. Accordingly, one can obtain an analytical expression for all the thermodynamic properties of the quantum liquid, including the equation of state [36, 39, 40, 61]. In particular, it can be shown that, for a Gaussian and harmonic PEL, the total energy of the system, $E(N, V, T) = (\partial(\beta F)/\partial\beta)_{N, V}$, is given by (see Appendix A)

$$E(N, V, T) = E_{IS}(N, V, T) + E_{vib}(N, V, T) \quad (14)$$

where

$$E_{IS}(N, V, T) \approx E_{IS}^{harm}(N, V, T) = E_0(V, T) - \sigma^2(V, T)(\beta + b) \quad (15)$$

and

$$E_{vib}(N, V, T) \approx E_{vib}^{harm}(N, V, T) = 3Nn_b k_B T + \left(\frac{\partial \mathcal{S}}{\partial \beta} \right)_{N, V, E_{IS}} \quad (16)$$

In Eq. 15, $b \equiv \left(\frac{\partial \mathcal{S}(N, V, T, e_{IS})}{\partial e_{IS}} \right)_{N, V, T, e_{IS}=E_{IS}}$. As explained in Ref. [42], to obtain Eqs. 15 and 16, we have assumed that the parameters $\alpha = \alpha(V)$, $E_0 = E_0(V)$, and $\sigma = \sigma(V)$, i.e., they are T -independent. We note that Eq. 15 and 16 are also valid for classical liquids. In the classical case, however, Eq. 16 reduces to $E_{vib} = 3Nk_B T$ since $n_b = 1$ and the last term of Eq. 16 vanishes (the PEL for classical system is T -independent). Alternatively, it can be shown that $\left(\frac{\partial \mathcal{S}(N, V, T, e_{IS})}{\partial \beta} \right)_{N, V, e_{IS}=E_{IS}} = E_{sp}(N, V, T)$ [see Appendix B] where $E_{sp}(N, V, T) \equiv \langle \sum_i \sum_k^{n_b} \frac{1}{2} k_i^{sp} (\mathbf{r}_i^{k+1} - \mathbf{r}_i^k)^2 \rangle_{N, V, T}$ is the potential energy of the ring-polymer *springs*. For classical systems, $n_b = 1$, (there are no springs associated to the liquid atoms) and hence, $E_{sp}(N, V, T) = 0$.

Relevant to this work, we note that Eqs. 15 and 16 hold for the case of *classical* LJBM [62, 63] suggesting that its PEL is indeed Gaussian and harmonic. In the

classical case, $E_{vib} = 3Nk_B T$ since the PEL and hence, S , are T -independent. Below we show that Eqs. 15 and 16 also hold for quantum LJBM if the Planck's constant is small (mild quantumness, $\hbar = \hbar_a$) but fail as the Planck's constant is increased. For large values of \hbar , anharmonic correction to the harmonic approximation of the PEL are needed.

3.2 Anharmonic Corrections in the PEL Formalism

Anharmonic corrections to the PEL have been introduced in the past to study the equation of state of *classical* liquids using the PEL formalism [28, 37, 39, 40]. In most studies, anharmonicities were assumed to depend only on T , implying that the basins anharmonicities were independent of where the basins were located within the PEL (the basins anharmonicities were assumed to be independent of the basin IS energy e_{IS}). Here, we present a general approach where the anharmonic corrections to the PEL may vary with both T and e_{IS} .

In the presence of anharmonic corrections, one can *formally* express the vibrational Helmholtz free energy of the system as

$$F_{vib}(N, V, T) = F_{vib}^{harm}(N, V, T) + F_{vib}^{anh}(N, V, T, E_{IS}), \quad (17)$$

where $F_{vib}^{harm}(N, V, T)$ is given by Eq. 11 and $F_{vib}^{anh}(N, V, T, E_{IS})$ is the correction due to the basins anharmonicity. The formal expression for the total energy of the system, $E(N, V, T) = (\partial \beta F(N, V, T) / \partial \beta)_{N, V}$, follows from Eqs. 13 and 17. It can be shown that $E(N, V, T)$ is also given by Eqn. 14, however, the new expressions for E_{IS} and E_{vib} (for a Gaussian PEL with anharmonic corrections) change as follows (see Appendix A).

$$E_{IS}(N, V, T) = E_{IS}^{harm}(N, V, T) + E_{IS}^{anh}(N, V, T) \quad (18)$$

where $E_{IS}^{harm}(N, V, T)$ is given by Eq. 15, and

$$E_{IS}^{anh}(N, V, T) = -\sigma^2 \left(\frac{\partial (\beta F_{vib}^{anh}(N, V, T, e_{IS}))}{\partial e_{IS}} \right)_{N, V, T, e_{IS}=E_{IS}}. \quad (19)$$

The new expression for E_{vib} is given by

$$E_{vib}(N, V, T) = E_{vib}^{harm}(N, V, T) + E_{vib}^{anh}(N, V, T, E_{IS}) \quad (20)$$

where $E_{vib}^{harm}(N, V, T)$ is given by Eq. 16, and

$$E_{vib}^{anh}(N, V, T) = \left(\frac{\partial (\beta F_{vib}^{anh}(N, V, T, E_{IS}))}{\partial \beta} \right)_{N, V, E_{IS}}. \quad (21)$$

Eqs. 19 and 21 are formal expressions that yield E_{IS}^{anh} and E_{vib}^{anh} once F_{vib}^{anh} is provided. As an example, we consider the case where the anharmonic corrections

depend only on T . In this case, one can write the following general expression, [28]

$$F_{vib}^{anh}(N, V, T, E_{IS}) = \sum_{i=2}^{i_{max}} \frac{c_i}{1-i} T^i, \quad (22)$$

where the coefficients $\{c_i\}$ depend only on (V, N) . In this case, Eq. 21 implies that

$$E_{vib}^{anh}(N, V, T) = \sum_{i=2}^{i_{max}} c_i T^i \quad (23)$$

while $E_{IS} = E_{IS}^{harm}$ (from Eq. 19, $E_{IS}^{anh} = 0$). Eqs. 22 and 23 are consistent with Refs. [39, 40].

In this work, we will model the anharmonicities of the PEL basins of the quantum LJBM as $\beta F_{vib}^{anh} = \sum_{i=1}^{\infty} \tilde{B}_i(N, V, T) e_{IS}^i$ where the coefficients $\tilde{B}_i(N, V, T)$ can be obtained from the RPMD simulations (see below). However, we find that keeping this expansion up to first order in e_{IS} is sufficient to fit the LJBM's studied in this work,

$$\beta F_{vib}^{anh}(N, V, T, e_{IS}) = \tilde{B}_0(N, V, T) + \tilde{B}_1(N, V, T) e_{IS} \quad (24)$$

Using Eqs. 19 and 21, one obtains

$$E_{IS}^{anh}(N, V, T) = -\sigma^2 \tilde{B}_1(N, V, T) \quad (25)$$

and

$$E_{vib}^{anh}(N, V, T, E_{IS}) = \left(\frac{\partial \tilde{B}_0(N, V, T)}{\partial \beta} \right)_{N, V} + \left(\frac{\partial \tilde{B}_1(N, V, T)}{\partial \beta} \right)_{N, V} E_{IS}(N, V, T) \quad (26)$$

To summarize, for a Gaussian PEL with anharmonicities given by Eq. 24, the following expressions hold (using Eqs. 17, 18, 20, 24, 25, 26),

$$F_{vib}(N, V, T, e_{IS}) = 3Nn_b k_B T \ln(\beta \hbar \omega_0) + k_B T \mathcal{S}(N, V, T, e_{IS}) + \tilde{B}_0(N, V, T) + \tilde{B}_1(N, V, T) e_{IS} \quad (27)$$

$$E_{IS}(N, V, T) = E_0(V) - \sigma(V)^2 \left(\beta + b(N, V, T) + \tilde{B}_1(N, V, T) \right) \quad (28)$$

$$E_{vib}(N, V, T) = 3Nn_b k_B T + \left(\frac{\partial \mathcal{S}(N, V, T, E_{IS})}{\partial \beta} \right)_{N, V, E_{IS}} + \left(\frac{\partial \tilde{B}_0(N, V, T)}{\partial \beta} \right)_{N, V} + \left(\frac{\partial \tilde{B}_1(N, V, T)}{\partial \beta} \right)_{N, V} E_{IS}(N, V, T) \quad (29)$$

3.3 Hypotheses and Protocols

The theoretical predictions of the PEL formalism (Sec. 3) are based on a handful of PEL variables, $\{\alpha, E_0, \sigma^2, b, \mathcal{S}, \tilde{E}_0, \tilde{B}_1\}$. For any practical purpose, these quantities need to be fit to properties obtained from the RPMD simulations. Next, we explain how these quantities are obtained, and the approximations involved.

Quantities $\{\mathcal{S}, b\}$. For the classical LJBM, the normal mode frequencies $\{\omega_{j,0}\}$ with $j = 1, 2, \dots, 3N$ are calculated by diagonalizing the corresponding *mass-weighted* Hessian matrix evaluated at the IS sampled by the system; the eigenvalues of the *mass-weighted* Hessian matrix are $\{(\omega_{j,0})^2\}$. For the quantum liquid/ring-polymer systems, there are $3n_b N$ normal mode frequencies $\{\omega_j\}$ ($j = 1, 2, \dots, 3n_b N$) given by the eigenvalues of the *mass-weighted* Hessian matrix of the ring-polymer system evaluated at the corresponding IS [Eq. 12]. In this case, we follow the procedure described in Refs. [13, 42] to obtain the ring-polymer (IS) normal mode frequencies analytically, using the values $\{\omega_{j,0}\}$ of the corresponding classical system; see Eq. 20 in Ref. [13].

The normal mode frequencies so obtained are then used in Eq. 12 to calculate the shape function of the system. As shown in the supplementary information (SI), and consistent with previous MD/PIMD studies of classical and quantum liquids, our path-integral computer simulations of the LJBM show that

$$\mathcal{S}(N, V, T, e_{IS}) \approx a(N, V, T) + b(N, V, T) e_{IS} \quad (30)$$

for all values of h studied. Note that for quantum liquids, the variables a and b depend on (N, V, T) while, in the classical case, they depend only on (N, V) .

Quantities $\{\alpha, E_0, \sigma^2\}$. These parameters characterize the configurational entropy of the system $S_{IS}(N, V, T, e_{IS})$ and hence, they specify how the IS are distributed within the PEL (Eqs. 9 and 10). In our previous studies [13, 42], we assumed that, for the quantum liquids, $\{\alpha, E_0, \sigma^2\}$ were independent of T . This implies that, while the PEL of the quantum liquid is T -dependent, the distribution of IS within the PEL is not.

In previous studies [13, 41, 42], we found that the Gaussian approximation of the PEL works remarkably well for atomistic and molecular quantum liquids. In the absence of anharmonicities, Eq. 15 was found to be in very good agreement with the values of $E_{IS}(T)$ obtained from RPMD simulations of an atomistic and molecular systems [13, 42]. Importantly, (i) it was found that the parameters $\{\alpha, E_0, \sigma^2\}$ (in the absence of anharmonicities) depend on the quantumness of the liquid (i.e., they all depend on h).

This is not unreasonable since, varying h , changes the Hamiltonian of the ring-polymer system (Eq. 4). However, we also found indications that the values of $\{\alpha, E_0, \sigma^2\}$ should *not* depend on the nature (classical/quantum) of the liquid (as quantified by h). Specifically, if the values of $\{\alpha, E_0, \sigma^2\}$ vary with h then the distributions of the IS in the PEL of classical and quantum liquids must be different. For this to be the case, there should be IS in the ring-polymer system PEL (RP-PEL) where the ring-polymers are *not* collapsed – as explained in Ref. [42], if the ring-polymers are collapsed at the IS of the RP-PEL then such IS (in the RP-PEL) also define an

IS of the classical liquid PEL (CL-PEL), and *vice versa* [42]. However, (ii) for all the quantum liquids studied [13, 41, 42], it was always found that the ring-polymers were collapsed at the IS of the RP-PEL sampled by the system.

There are two options for the findings (i) and (ii) to be compatible. (A) One may assume that the quantities $\{\alpha, E_0, \sigma^2\}$ vary with the quantumness of the liquid *but* the IS of the RP-PEL with *non-collapsed* ring-polymers are rare, difficult to sample in the RPMD simulations. Alternatively, one may consider that (B) there are no IS in the RP-PEL where ring-polymers are not collapsed at the working conditions and hence, the quantities $\{\alpha, E_0, \sigma^2\}$ are independent of whether the liquid obeys classical or quantum mechanics. In this work, we will assume that option (B) holds. Accordingly, the values of $\{\alpha, E_0, \sigma^2\}$ are considered to be \hbar -independent and hence, they will be extracted from the classical MD simulations, following the same procedure from previous classical MD simulations [39, 40, 43, 46, 63]. It follows from Eq. 10, that hypothesis (B) also implies that the configurational entropy S_{IS} of the system as a function of e_{IS} is identical for the classical and quantum liquid. As we will show, in the scenario (B), anharmonicities may need to be included.

Quantities $\{\tilde{B}_0, \tilde{B}_1\}$. As a general expressions, we will consider that, for fix value of (N, V) ,

$$\tilde{B}_j(T) = \sum_{i=0}^{i_{max}} c_{j,i} T^i \quad (31)$$

where $j = 0, 1$. We find that a value of $i_{max} = 3$ is sufficient to reproduce the results from the RPMD simulations. As will be shown below, the coefficients $c_{j=1,i}$ can be obtained from the RPMD simulations using Eq. 25. Similarly, the coefficient $c_{j=0,i}$ can be obtained from the RPMD simulations using Eq. 26 (the constant $c_{0,0}$ cannot be obtained in this way but plays no role in the configurational entropy S_{IS} , since it is an additive constant in the total free energy of the system).

In order to validate hypothesis (B), in Sec. 4 we will test whether the configurational entropy given in Eq. 10, with the parameters $\{\alpha, E_0, \sigma^2\}$ of the classical LJBMs, also hold for the quantum LJBMs studied. To do so, we note that the probability for the system to sample a basin with IS energy e_{IS} , at a given T (N, V are constant) is given by

$$P(e_{IS}, T) = \frac{e^{-\beta(e_{IS} - TS_{IS}(N, V, T, e_{IS}) + F_{vib}(N, V, T, e_{IS}))}}{Q(N, V, T)} \quad (32)$$

Accordingly, $S_{IS}(N, V, T, e_{IS})$ must obey the following expression (see Eqs. 11 and 17),

$$\begin{aligned} S_{IS}(N, V, T, e_{IS})/k_B &= \ln(P(e_{IS}, T)) + 3Nn_b \ln(\beta\hbar\omega_0) \\ &+ \mathcal{S}(N, V, T, e_{IS}) + \beta e_{IS} + \beta F_{vib}^{anh}(N, V, T, e_{IS}) + \ln(Q(N, V, T)) \end{aligned} \quad (33)$$

In this work, we will calculate $P(e_{IS}, T)$ directly from RPMD simulations of LJBM and use Eq. 33 to validate the expression for $S_{IS}(N, V, T, e_{IS})$ obtained from the PEL formalism (with the hypothesis (B) discussed above).

4 Potential Energy Landscape of *classical* and *quantum* Lennard-Jones Binary Mixtures

Equilibrium properties. We focus on the total energy $E(T)$ and pressure $P(T)$ of the LJBM with different levels of quantumness. Figs. 1(a) and 1(b) show $E(T)$ and $P(T)$ for the LJBM obtained from MD/PMD simulations with $h = 0$ (classical) and $h = h_a, h_b, h_c$ (quantum). At high temperatures the values of $E(T)$ and $P(T)$ obtained for different values of h become closer and closer with increasing temperatures. Hence, quantum effects do not affect the thermodynamic properties of the LJBM at very high temperatures (as expected). Instead, at low temperatures ($T < 1.0$), both $E(T)$ and $P(T)$ increase with increasing h , as the LJBM become more quantum. This is due to the quantum delocalization of the atoms which becomes more pronounced with increasing h . Indeed, as shown in Fig. 1(c), the radius of gyration, $R_g(T)$, of the ring-polymers associated to the LJBM increases with increasing h . We note that the atoms delocalization in the LJBM studied is mild but not negligible. At the lowest temperatures studied, $R_g \lesssim 0.09$; a value of $R_g = 0.09$ indicates that the ring-polymers expand over a sphere of radius approximately equal to 9% of the A-particle hard-core radius.

PEL of the LJBM. The IS and vibrational energy of the studied LJBM, $E_{IS}(T)$ and $E_{vib}(T)$, are included in Fig. 2(a)(b). The results from the RPMD simulations are indicated by circles; the lines are the prediction using Eqs 15 and 16 for the case where the PEL of the classical/quantum LJBM are assumed to be Gaussian and *harmonic*. As explained in Sec. 3.3, we consider that the distribution of IS in the CL-PEL and RP-PEL are identical, i.e., in both cases, Ω_{IS} is given by Eq. 9 with the *same* values of $\{\alpha, E_0, \sigma^2\}$. It follows from Fig. 2(a)(b) that, when nuclear quantum effects are small ($h = 0, h_a$), the Gaussian and harmonic approximation of the PEL are fully consistent with the RPMD simulations of the LJBM. However, as the quantum nature of the LJBM increases ($h = h_b, h_c$), deviations between the predictions of the PEL formalism (within the Gaussian and harmonic approximation of the PEL, Eqs 15 and 16) and RPMD simulations become evident in both $E_{IS}(T)$ and $E_{vib}(T)$. Accordingly, for $h = h_b, h_c$, anharmonic corrections are needed.

The anharmonic corrections to $E_{IS}(T)$ and $E_{vib}(T)$ can be calculated numerically from Figs. 2(a)(b) and using the expressions $E_{IS}^{anh}(T) = E_{IS}(T) - E_{IS}^{harm}(T)$ and $E_{vib}^{anh}(T) = E_{vib}(T) - E_{vib}^{harm}(T)$. The so-obtained values of $E_{IS}^{anh}(T)$ and $E_{vib}^{anh}(T)$ are indicated by circles in Fig. 2(c)(d). Also included in Figs. 2(c)(d) are the fits to $E_{IS}^{anh}(T)$ and $E_{vib}^{anh}(T)$ using Eqs. 25 and 26, respectively, and Eq. 31 (lines). The fits to the data points in Figs. 2(c)(d) are excellent indicating that, for the LJBM studied, the anharmonic contributions to the vibrational free energy can indeed be modeled using Eq. 24 with the coefficients \tilde{B}_j given by Eq. 31. The coefficients B_0 and B_1 are shown in Fig. 3.

For comparison, we include in Fig. 4 the values of $E_{IS}(T)$ and $E_{vib}(T)$ obtained numerically (taken from Fig. 2(a)(b); circles) together with the corresponding predictions of the PEL formalism *including* the anharmonic corrections; see Eqs. 28 and 29. The agreement between the predictions of the PEL formalism (with the Gaussian approximation and including anharmonicities) and RPMD simulations is excellent. Accordingly, for the case of the LJBM studied, one can model the anharmonicities of the PEL as indicated by Eqs. 24 and 31. Importantly, Fig. 4 also supports strongly that hypothesis (B) indeed holds for the case of the LJBM studied.

Configurational Entropy. Next, we study the configurational entropy of the quantum LJBM. We also test whether the hypotheses of this work are self-consistent within the PEL formalism. Specifically, our results are based on the hypotheses that (i) $\Omega_{IS}(e_{IS})$ is identical for the classical and quantum liquids (given by the Gaussian approximation, Eq. 9, with identical PEL variables $\{\alpha, E_0, \sigma^2\}$), and that (ii) the PEL anharmonicities can be modeled using Eq. 24.

Hypothesis (i) implies that for all the LJBM studied, $S_{IS}(N, V, T, e_{IS}) = S_{IS}(N, V, e_{IS})$, independent of h , with $S_{IS}(N, V, e_{IS})$ given by Eq. 10. Again, this implies that, *at a given depth e_{IS} of the corresponding PEL*, the classical and quantum liquids have access to the same number of IS [Fig. 5(a) shows the $S_{IS}(N, V, e_{IS})$ of the LJBM as a function of e_{IS}]. However, the number of IS accessible to the LJBM *at a given temperature* does depend on the quantumness of the LJBM considered. To show this, we include in Fig. 5(b), S_{IS} as a function of T , after substituting $E_{IS}(T)$ using Eq. 28. Since $E_{IS}(T)$ varies with h (Fig. 4), the temperature-dependence of S_{IS} is different for the LJBM studied. Our RPMD simulations show that S_{IS} shifts towards higher temperatures as h increases. In particular, the Kauzmann temperature T_K , defined as the temperature at which $S_{IS} = 0$, increases considerably as the liquid becomes more quantum. Specifically, $T_K = 0.291, 0.319, 0.355, 0.406$ for $h = 0, h_a, h_b, h_c$, respectively. Overall, our results imply that, *at a given temperature*, the LJBM explore IS located at different depths of the corresponding PEL (Fig. 4) and hence, they have access to a different number of IS in the corresponding PEL (Fig. 5(b)).

To confirm that the calculated configurational entropy of the LJBM (Fig. 5) are physically sound (i.e., self-consistent with the PEL formalism), we test that our results are consistent with Eq. 33. A similar self-consistency test was implemented for the case of the classical LJBM in Ref. [62, 63]. Eq. 33 imposes a strict relationship between the $S_{IS}(N, V, e_{IS})$ and the probability distribution $P(e_{IS}, T)$. Specifically, at fixed (N, V) , the PEL formalism (Eq. 33) requires that

$$S_{IS}(T, e_{IS})/k_B = \ln(P(T, e_{IS})) + 3Nn_b \ln(\beta\hbar\omega_0) + \mathcal{S}(T, e_{IS}) + \beta e_{IS} + \beta F_{vib}^{anh}(T, e_{IS}) + c(T) \quad (34)$$

where $c(T)$ is a quantity independent of e_{IS} . Accordingly, independently of the temperature considered, the right-hand-side of Eq. 34 should overlap with $S_{IS}(N, V, e_{IS})$ (up to some function $c(T)$). We note that $P(T, e_{IS})$ is calculated numerically from the RPMD simulations and hence, Eq. 34 provides a strong test to the validity of the $S_{IS}(N, V, e_{IS})$ reported in this work as well as to the underlying hypotheses (i) and (ii)

stated above. Fig. 6 shows the $S_{IS}(N, V, e_{IS})$ of the LJBMs for $h = h_a, h_b, h_c$ [black line; taken from Fig. 5(a)] together with the corresponding fit given by the right-hand-side of Eq. 34 (the value of $c(T)$ is adjusted for a maximum overlap between both sides of Eq. 34) [63]. It follows from Figure 6 that Eq. 34 holds remarkably well up to approximately $T = 1.0$, which is a rather high temperature for the LJBMs studied.

Adam-Gibbs Relation The Adam-Gibbs relation relates the diffusion coefficient $D(T)$ of a liquid with its configurational entropy as follows [6],

$$D(T) = D_0 \exp(-A/TS_{IS}) \quad (35)$$

where D_0 and A are constants. Eq. 35 implies that the diffusivity at a given temperature is controlled by the corresponding number of IS available to the system in the PEL, i.e., the topography of the PEL controls the dynamics of the liquid of interest. Eq. 35 has been validated in computational studies of diverse classical liquids, including silica [32] and water [47]. Here, we show that the Eq. 35 also holds for the LJBMs studied, independently of the quantum character (h) of the mixtures.

The diffusion coefficient is calculated from the mean-square displacement (MSD) of the ring-polymer centroids as a function of time. Specifically, for an atomistic liquid, $\text{MSD}(t) \approx 6Dt$ at long-times [64]. Fig. 7 shows the so-obtained values of $D(T)$ as a function $1/TS_{IS}(T)$ for all the LJBMs studied [circles; S_{IS} is taken from Fig. 5(b)]. The solid lines are the linear fits to the data points using Eq. 35. The agreement between the RPMD simulations and the Adam-Gibbs equation is remarkable good, extending for approximately four orders of magnitude in D .

5 Summary and Discussion

One of the main goals of this work is to show that, from a thermodynamic/statistical mechanics point of view, the PEL formalism provides a unifying description of classical and quantum liquids over a wide range of temperatures down to the glass state. In the classical case, the PEL of a liquid is given by the potential energy function of the system as a function of the atoms coordinates, $U(\mathbf{r}_1, \mathbf{r}_2, \dots, \mathbf{r}_N)$, and the system is represented by a point moving on such a PEL (CL-PEL). In the quantum case, one can associate the PEL of the underlying ring-polymer system (RP-PEL) to the quantum liquid (for a fix number of beads per ring-polymer, n_b). As discussed in this work, the PEL associated to the quantum liquid is defined by Eq. 5, and the quantum liquid, again, can be represented by a point moving on the so-defined RP-PEL. Therefore, independently of whether the system obeys classical or quantum mechanics, the *liquid* is characterized by a point that describes a trajectory on the corresponding CL-PEL/RP-PEL as the system visits different basins over time. In the *glass* state, the representative point of the system would be limited to vibrational motion within a single basin of the CL-PEL/RP-PEL as molecules/atoms are unable to diffuse.

Building upon the similarities between classical and quantum liquids in the PEL formalism, we show that the RP-PEL can be used to define a configurational entropy that can be associated to the quantum liquid in a precise manner. As for the classical case, $S_{IS}(N, V, T)$ is a measure of the number of IS available to the ring-polymer

system associated to the quantum liquid (Eq. 10). Importantly, using the so-defined configurational entropy, it is shown that one can also extend the Adam-Gibbs relation to the quantum case. This implies that the dynamics of the quantum liquid is controlled by the number of IS available to the ring-polymer system at a given (N, V, T) [Fig. 7]. It follows that the configurational entropy associated to the quantum liquid has a physical relevance from the dynamical point of view.

The configurational entropy defined in this work is based on the hypothesis that (A) the distribution of IS, Ω_{IS} , at a given working conditions (N, V, T) , is identical for the classical and quantum liquid. Within the Gaussian approximation of the PEL (Eq. 9), which is valid for the studied LJBM (Fig. 4), this also implies that the PEL quantities $\{\alpha, E_0, \sigma^2\}$ do not depend on the nature (quantum/classical) of the liquid studied, and that they depend only on V (but not on T). Accordingly, the CL-PEL and RP-PEL have the same number of IS at a given IS energy/PEL depth. Hence, from a practical point of view, the PEL quantities $\{\alpha, E_0, \sigma^2\}$ can be calculated from classical MD simulations (as opposed to the more computationally expensive path-integral computer simulations). We stress that, as shown in Fig. 6, the so-obtained $S_{IS}(N, V, T)$ is validated by testing that Eq. 33 is in agreement with the RPMD simulations of the LJBM. It follows that hypothesis (A) is self-consistent within the PEL formalism. As explained in this work, hypothesis (A) should hold as far as the ring-polymers associated to the quantum liquid collapse at the sampled IS. This seems to be rather general for systems where the NQE (atoms delocalization) are mild; indeed, PIMD simulations of water [13], monatomic quantum liquids [41, 42, 65], and LJBM (this work) at low temperatures show no sign of delocalized ring-polymers at the corresponding IS.

Our study emphasizes the role of anharmonic contributions in the PEL formalism. For the case of the LJBM with non-negligible quantumness ($h > h_a$), our RPMD simulations indicate that hypothesis (A) requires the inclusion of anharmonicities in the PEL-based description (Fig. 2). Accordingly, in this study, we also provide a general approach to include anharmonicities. In this regard, we note that Eqs. 19 and 21 define unequivocally the *anharmonic* Helmholtz free energy since these are two independent equations that define the two partial derivatives of $F_{vib}^{anh}(N, V, T, e_{IS})$ (at fixed (N, V)). Our RPMD simulations based on the LJBM show that while the PEL of the classical and weakly-quantum LJBM are harmonic ($h \leq h_a$), anharmonicities become increasingly relevant with increasing h ($h > h_a$).

Being able to extend the PEL formalism to low-temperature liquids/glasses that obey quantum mechanics provides a simple tool to explore the role of quantum mechanics on atomistic liquids composed of light-element as well as molecular liquids composed of small molecules that contain H atoms, such as water. In these cases, NQE can play a relevant role even at non-negligible temperatures (e.g., $T \approx 80 - 270$ K) [66]. Extending the concept of configurational entropy to quantum liquids is fundamental in providing a thermodynamic description of liquids that obey quantum mechanics. For example, it may be possible to write an equation of state for quantum liquids using the PEL formalism by following a procedure similar to that used in the case of classical liquids [36, 39].

6 Data Availability

The authors confirm that the data supporting the findings of this study are available within the article and its supplementary material.

7 Acknowledgments

This work was supported by the NSF CREST Center for Interface Design and Engineered Assembly of Low Dimensional systems (IDEALS), NSF grant number HRD-1547380. This work was also supported by the Advanced Cyberinfrastructure Coordination Ecosystem: Services & Support (ACCESS) program [67], which is supported by the National Science Foundation Grant Nos. 2138259, 2138286, 2138307, 2137603, and 213829669.

8 Additional Information

The authors declare no conflict of interest.

9 Supplementary Information

In the Supplementary Information, we demonstrate the importance of the anharmonic contributions of the PEL by comparing the configurational entropy of LJBMs (Fig. 5) using Eq. 33 but omitting the anharmonic term F_{vib}^{anh} . Our result shows that the anharmonic term F_{vib}^{anh} becomes significant for systems with stronger quantumness (h_b, h_c). The SI also includes results from RPMD simulations showing that Eq. 30 holds for the LJBMs studied.

10 Figures

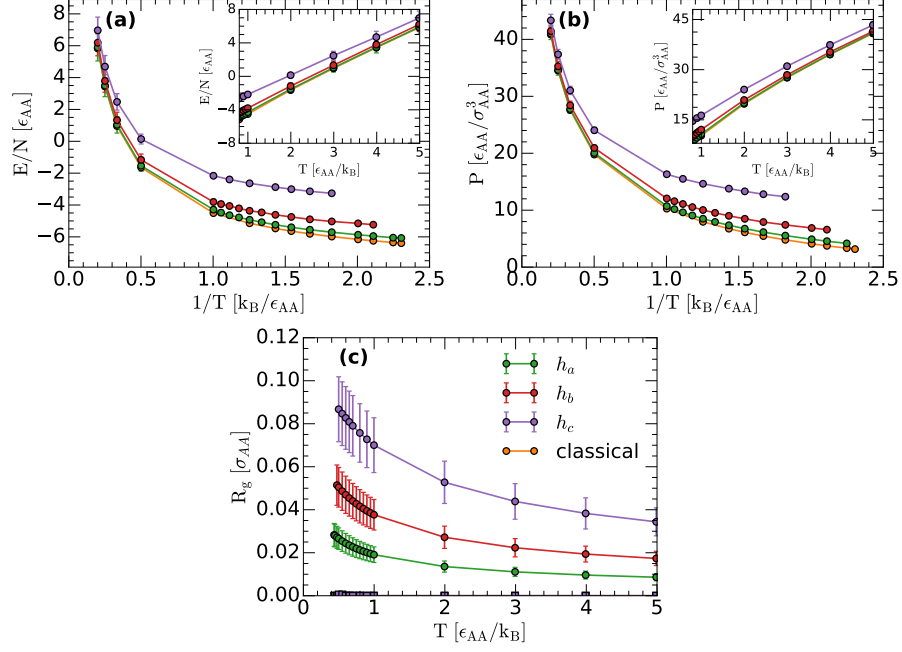


Fig. 1 (a) Total energy and (b) pressure of the LJBMs as a function of temperature ($\rho = 1.2$) obtained from RPMD simulations with Planck's constant $h = 0$ (classical), $h_a = 0.2474$, $h_b = 0.5$, and $h_c = 0.7948$. As h increases, and the LJBMs become more quantum, both $E(T)$ and $P(T)$ increase, particularly at low temperatures. (c) Radius of gyration R_g of the A-type particles of the LJBMs studied (circles). In all cases, $R_g(T)$ increases upon cooling. The observed atoms delocalization becomes more pronounced with increasing h . The squares in (c) correspond to the values of R_g at the IS sampled by the system; $R_g(T) \approx 0$ at the IS implying that the ring-polymers are collapsed.

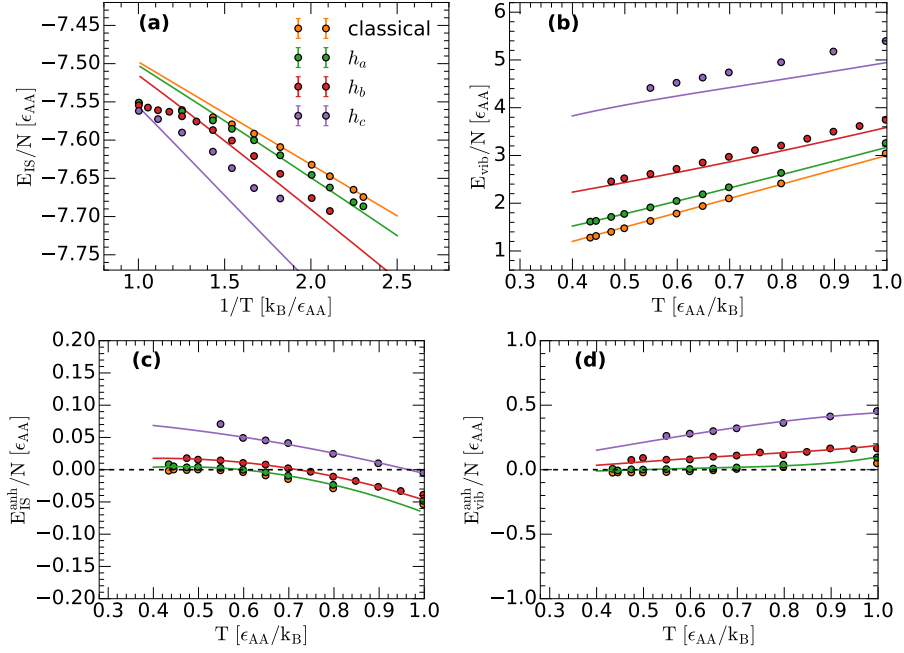


Fig. 2 (a) Inherent structure energy $E_{IS}(T)$ and (b) vibrational energy $E_{vib}(T)$ as a function of temperature for the LJBMJs studied. Results are obtained from RPMD simulations using a Planck's constant $\hbar = 0$ (i.e., classical MD simulations), and $\hbar = h_a, h_b, h_c$ (circles). Lines are the predictions of the PEL formalism for a Gaussian and harmonic PEL, $E_{IS}^{harm}(T)$ and $E_{vib}^{harm}(T)$, given in Eqs. 15 and 16. (c) Anharmonic contributions to the IS energy, $E_{IS}^{anh}(T) = E_{IS}(T) - E_{IS}^{harm}(T)$, obtained from (a) [circles]. Lines are the fit to the data points using Eq. 25 and 31. (d) Anharmonic contributions to the vibrational energy, $E_{vib}^{anh}(T) = E_{vib}(T) - E_{vib}^{harm}(T)$, obtained from (b) [circles]. Lines are the fit to the data points using Eq. 26 and 31. Anharmonicities are relevant for $\hbar = h_b, h_c$ but not for $\hbar = 0, h_a$. Dashed-lines in (c)(d) correspond to zero energy.

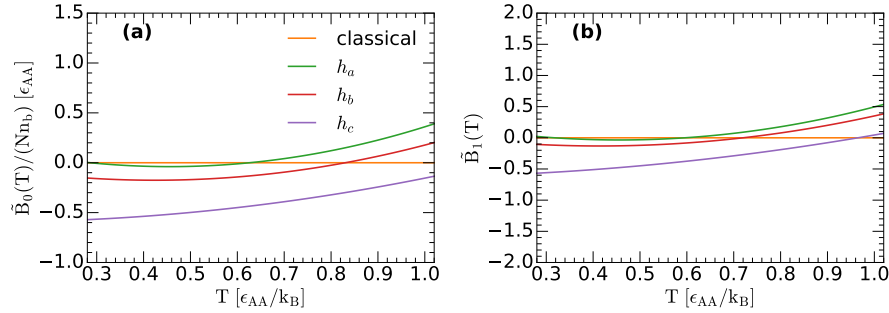


Fig. 3 Coefficient \tilde{B}_0 and \tilde{B}_1 defined in Eq. 24 and obtained from the fittings in Figs. 2(c)(d).

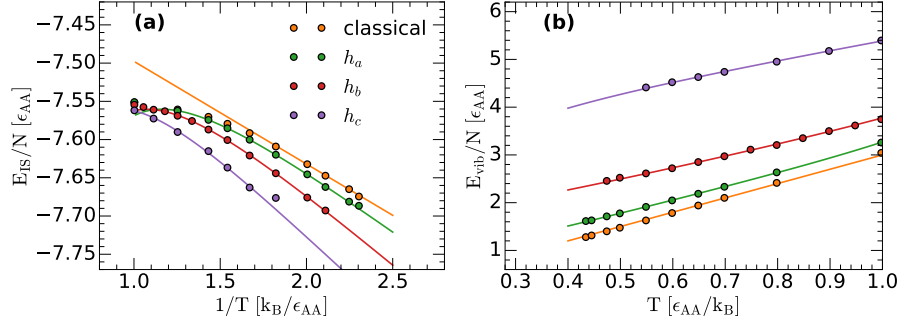


Fig. 4 (a) Inherent structure energy $E_{IS}(T)$ and (b) vibrational energy $E_{vib}(T)$ as a function of temperature for the LJBM systems studied. Results are obtained from RPMD simulations [circles; taken from Figs. 2(a) and 2(b)]. Lines are the fit to the data using the predictions of the PEL formalism for a Gaussian and anharmonic PEL, using Eqs. 28 and 29 (see text).

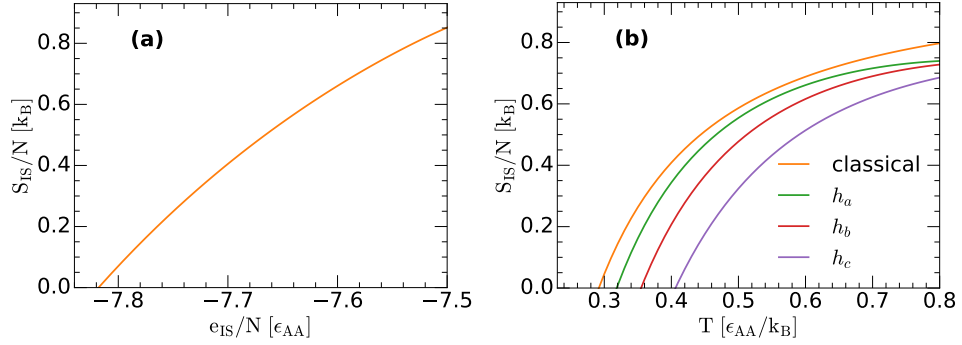


Fig. 5 (a) Configurational entropy as a function of the IS energy, $S_{IS}(e_{IS})$, for the classical and quantum LJBM systems studied [Eq. 10]; $S_{IS}(e_{IS})$ is independent of the quantum character of the LJBM considered (see text). (b) Configurational entropy as a function of temperature, $S_{IS}(T) = S_{IS}(E_{IS}(T))$. The $S_{IS}(T)$ for the LJBM systems studied are obtained from (a) [Eq. 10] and using Eq. 28.

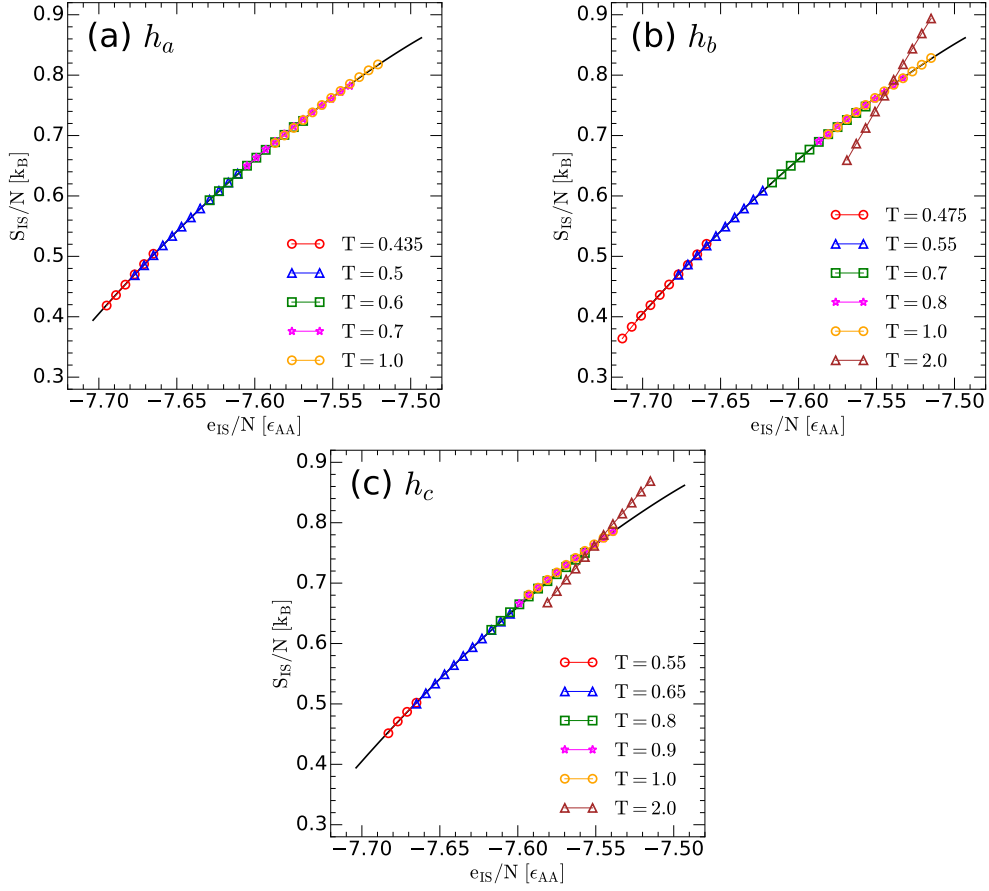


Fig. 6 Validation of the configurational entropy for the LJBM. (a) Configurational entropy of the LJBM as a function of the IS energy e_{IS} , $S_{IS}(e_{IS})$ [solid black line; taken from Fig. 5(a)]. The symbols correspond to the expression on the right-hand-side of Eq. 34 for temperatures $T = 0.435$ (red circles), 0.5 (blue up-triangles), 0.6 (green squares), 0.7 (magenta stars) and 1.0 (orange circles). Results at the different temperatures are obtained from RPMD simulations with $h = h_a$ [datasets are shifted by a constant $c(T)$; see text]. (b) Same as (a) for $h = h_b$, and for temperatures $T = 0.475$ (red circles), 0.55 (blue up-triangles), 0.7 (green squares), 0.8 (magenta stars), 1.0 (orange circles), and 2.0 (maroon up-triangles). (c) Same as (a) for $h = h_c$, and for temperatures $T = 0.55$ (red circles), 0.65 (blue up-triangles), 0.8 (green squares), 0.9 (magenta stars), 1.0 (orange circles), and 2.0 (maroon up-triangles). In all cases, the symbols fully overlap with the black line at low temperatures ($T \leq 1.0$), implying that Eq. 34 holds. At higher temperatures, deviations from Eq. 34 become evident [see, maroon up-triangles in (b) and (c) for the case $T = 2.0$]

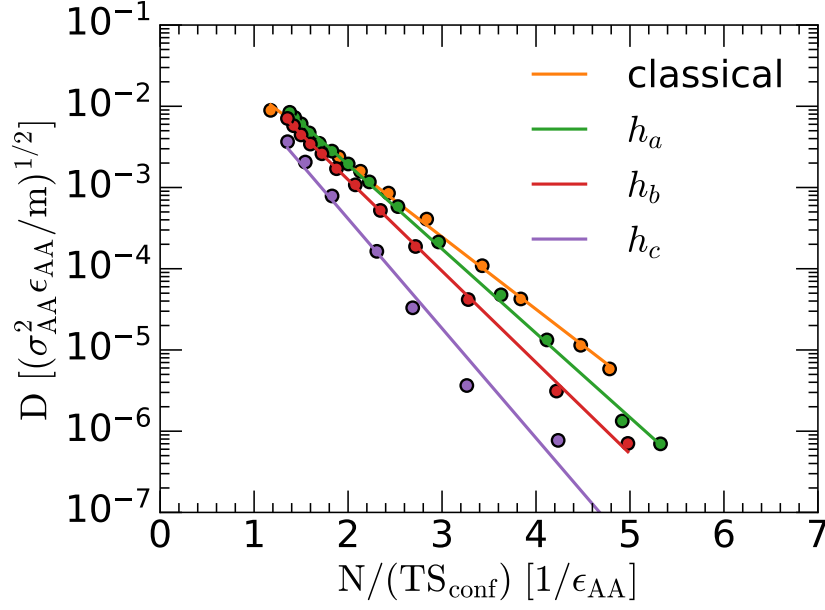


Fig. 7 Diffusion coefficient of the LJBM studied obtained from RPMD simulations using $\hbar = 0$ (classical MD), and $\hbar = \hbar_a, \hbar_b, \hbar_c$ (circles). Lines are the Adam-Gibbs prediction (Eq. 35) with the configurational entropies S_{IS} given in Fig. 5(b). The Adam-Gibbs relation holds for all the classical and quantum LJBM studied for over more than four decades in D .

References

- [1] Angell, C. A. Formation of Glasses from Liquids and Biopolymers. *Science* **267**, 1924–1935 (1995).
- [2] Debenedetti, P. G. & Stillinger, F. H. Supercooled liquids and the glass transition. *Nature* **410**, 259–267 (2001).
- [3] Binder, K. & Kob, W. *Glassy Materials and Disordered Solids: An Introduction to Their Statistical Mechanics* Rev. ed edn (World Scientific, Hackensack, NJ ; London ; Singapore, 2011).
- [4] Berthier, L. & Ediger, M. D. Facets of glass physics. *Physics Today* **69**, 40–46 (2016).
- [5] Kauzmann, Walter. The Nature of the Glassy State and the Behavior of Liquids at Low Temperatures. *Chemical Reviews* **43**, 219–256 (1948).
- [6] Adam, G. & Gibbs, J. H. On the Temperature Dependence of Cooperative Relaxation Properties in Glass-Forming Liquids. *The Journal of Chemical Physics* **43**, 139–146 (1965).
- [7] Ediger, M. D. Spatially Heterogeneous Dynamics in Supercooled Liquids. *Annual Review of Physical Chemistry* **51**, 99–128 (2000).
- [8] Schoenholz, S. S., Cubuk, E. D., Sussman, D. M., Kaxiras, E. & Liu, A. J. A structural approach to relaxation in glassy liquids. *Nature Physics* **12**, 469–471 (2016).
- [9] Bengtzelius, U., Gotze, W. & Sjolander, A. Dynamics of supercooled liquids and the glass transition. *Journal of Physics C: Solid State Physics* **17**, 5915–5934 (1984).
- [10] Kirkpatrick, T. R., Thirumalai, D. & Wolynes, P. G. Scaling concepts for the dynamics of viscous liquids near an ideal glassy state. *Physical Review A* **40**, 1045–1054 (1989).
- [11] Parisi, G. & Zamponi, F. Mean-field theory of hard sphere glasses and jamming. *Reviews of Modern Physics* **82**, 789–845 (2010).
- [12] Berthier, L. & Biroli, G. Theoretical perspective on the glass transition and amorphous materials. *Reviews of Modern Physics* **83**, 587–645 (2011).
- [13] Eltareb, A., Zhou, Y., Lopez, G. E. & Giovambattista, N. Potential energy landscape formalism for quantum molecular liquids. *Communications Chemistry* **7**, 289 (2024).

- [14] Gainaru, C. *et al.* Anomalous large isotope effect in the glass transition of water. *Proceedings of the National Academy of Sciences* **111**, 17402–17407 (2014).
- [15] Giubertoni, G., Bonn, M. & Woutersen, S. D₂O as an Imperfect Replacement for H₂O: Problem or Opportunity for Protein Research? *The Journal of Physical Chemistry B* **127**, 8086–8094 (2023).
- [16] Morales, M. A., Pierleoni, C., Schwegler, E. & Ceperley, D. M. Evidence for a first-order liquid-liquid transition in high-pressure hydrogen from ab initio simulations. *Proceedings of the National Academy of Sciences* **107**, 12799–12803 (2010).
- [17] Kinugawa, K. & Takemoto, A. Quantum polyamorphism in compressed distinguishable helium-4. *The Journal of Chemical Physics* **154**, 224503 (2021).
- [18] Tsujimoto, M. & Kinugawa, K. Two liquid states of distinguishable helium-4: The existence of another non-superfluid frozen by heating. *The Journal of Chemical Physics* **161**, 044501 (2024).
- [19] Amir, A., Oreg, Y. & Imry, Y. Slow Relaxations and Aging in the Electron Glass. *Physical Review Letters* **103**, 126403 (2009).
- [20] Müller, M. & Ioffe, L. B. Glass Transition and the Coulomb Gap in Electron Glasses. *Physical Review Letters* **93**, 256403 (2004).
- [21] Wu, W., Ellman, B., Rosenbaum, T. F., Aeppli, G. & Reich, D. H. From classical to quantum glass. *Physical Review Letters* **67**, 2076–2079 (1991).
- [22] Harris, R. *et al.* Phase transitions in a programmable quantum spin glass simulator. *Science* **361**, 162–165 (2018).
- [23] Charbonneau, P. *et al.* *Spin Glass Theory and Far Beyond: Replica Symmetry Breaking After 40 Years* (WORLD SCIENTIFIC, 2023).
- [24] Markland, T. E. *et al.* Quantum fluctuations can promote or inhibit glass formation. *Nature Physics* **7**, 134–137 (2011).
- [25] Klemm, R. A. Quantum effects in spin glasses. *Journal of Physics C: Solid State Physics* **12**, L735 (1979).
- [26] Stillinger, F. H. & Weber, T. A. Hidden structure in liquids. *Physical Review A* **25**, 978–989 (1982).
- [27] Stillinger, F. H. *Energy Landscapes, Inherent Structures, and Condensed-Matter Phenomena* (Princeton University Press, 2015).
- [28] Sciortino, F. Potential energy landscape description of supercooled liquids and glasses. *Journal of Statistical Mechanics: Theory and Experiment* **2005**, P05015 (2005).

- [29] Heuer, A. Exploring the potential energy landscape of glass-forming systems: From inherent structures via metabasins to macroscopic transport. *Journal of Physics: Condensed Matter* **20**, 373101 (2008).
- [30] Wales, D. J. Exploring Energy Landscapes. *Annual Review of Physical Chemistry* **69**, 401–425 (2018).
- [31] Sastry, S., Debenedetti, P. G. & Stillinger, F. H. Signatures of distinct dynamical regimes in the energy landscape of a glass-forming liquid. *Nature* **393**, 554–557 (1998).
- [32] Saika-Voivod, I., Sciortino, F. & Poole, P. H. Free energy and configurational entropy of liquid silica: Fragile-to-strong crossover and polyamorphism. *Physical Review E* **69**, 041503 (2004).
- [33] Zhou, Y., Lopez, G. E. & Giovambattista, N. Anomalous properties in the potential energy landscape of a monatomic liquid across the liquid–gas and liquid–liquid phase transitions. *The Journal of Chemical Physics* **157**, 124502 (2022).
- [34] Starr, F. W. *et al.* Thermodynamic and structural aspects of the potential energy surface of simulated water. *Physical Review E* **63**, 041201 (2001).
- [35] La Nave, E., Mossa, S., Sciortino, F. & Tartaglia, P. Liquid stability in a model for ortho-terphenyl. *The Journal of Chemical Physics* **120**, 6128–6134 (2004).
- [36] Roberts, C. J., Debenedetti, P. G. & Stillinger, F. H. Equation of State of the Energy Landscape of SPC/E Water. *The Journal of Physical Chemistry B* **103**, 10258–10265 (1999).
- [37] La Nave, E., Mossa, S. & Sciortino, F. Potential Energy Landscape Equation of State. *Physical Review Letters* **88**, 225701 (2002).
- [38] Shell, M. S., Debenedetti, P. G., La Nave, E. & Sciortino, F. Energy landscapes, ideal glasses, and their equation of state. *The Journal of Chemical Physics* **118**, 8821–8830 (2003).
- [39] Handle, P. H. & Sciortino, F. Potential energy landscape of TIP4P/2005 water. *The Journal of Chemical Physics* **148**, 134505 (2018).
- [40] Eltareb, A., Lopez, G. E. & Giovambattista, N. Potential energy landscape of a flexible water model: Equation of state, configurational entropy, and Adam–Gibbs relationship. *The Journal of Chemical Physics* **160**, 154510 (2024).
- [41] Giovambattista, N. & Lopez, G. E. Potential energy landscape formalism for quantum liquids. *Physical Review Research* **2**, 043441 (2020).
- [42] Zhou, Y., Lopez, G. E. & Giovambattista, N. The Harmonic and Gaussian Approximations in the Potential Energy Landscape Formalism for Quantum

- Liquids. *Journal of Chemical Theory and Computation* (2024).
- [43] Sastry, S. The relationship between fragility, configurational entropy and the potential energy landscape of glass-forming liquids. *Nature* **409**, 164–167 (2001).
 - [44] Berthier, L., Ozawa, M. & Scalliet, C. Configurational entropy of glass-forming liquids. *The Journal of Chemical Physics* **150**, 160902 (2019).
 - [45] Parisi, G., Urbani, P. & Zamponi, F. *Theory of Simple Glasses: Exact Solutions in Infinite Dimensions* (Cambridge University Press, New York, 2019).
 - [46] Scala, A., Starr, F. W., La Nave, E., Sciortino, F. & Stanley, H. E. Configurational entropy and diffusivity of supercooled water. *Nature* **406**, 166–169 (2000).
 - [47] Handle, P. H. & Sciortino, F. The Adam–Gibbs relation and the TIP4P/2005 model of water. *Molecular Physics* **116**, 3366–3371 (2018).
 - [48] Kob, W. & Andersen, H. C. Testing mode-coupling theory for a supercooled binary Lennard-Jones mixture. II. Intermediate scattering function and dynamic susceptibility. *Physical Review E* **52**, 4134–4153 (1995).
 - [49] Sciortino, F. & Tartaglia, P. Extension of the Fluctuation-Dissipation Theorem to the Physical Aging of a Model Glass-Forming Liquid. *Physical Review Letters* **86**, 107–110 (2001).
 - [50] Berthier, L. & Reichman, D. R. Modern computational studies of the glass transition. *Nature Reviews Physics* **5**, 102–116 (2023).
 - [51] Eastman, P. *et al.* OpenMM 7: Rapid development of high performance algorithms for molecular dynamics. *PLOS Computational Biology* **13**, e1005659 (2017).
 - [52] Craig, I. R. & Manolopoulos, D. E. Quantum statistics and classical mechanics: Real time correlation functions from ring polymer molecular dynamics. *The Journal of Chemical Physics* **121**, 3368–3373 (2004).
 - [53] Rossi, M., Ceriotti, M. & Manolopoulos, D. E. How to remove the spurious resonances from ring polymer molecular dynamics. *The Journal of Chemical Physics* **140**, 234116 (2014).
 - [54] Markland, T. E. *et al.* Theory and simulations of quantum glass forming liquids. *Journal of Chemical Physics* **136**, 074511–074511 (2012).
 - [55] Miller, T. F. Isomorphic classical molecular dynamics model for an excess electron in a supercritical fluid. *The Journal of Chemical Physics* **129**, 194502 (2008).
 - [56] Virtanen, P. *et al.* SciPy 1.0: Fundamental algorithms for scientific computing in Python. *Nature Methods* **17**, 261–272 (2020).

- [57] Harris, C. R. *et al.* Array programming with NumPy. *Nature* **585**, 357–362 (2020).
- [58] Tuckerman, M. E. *Statistical Mechanics: Theory and Molecular Simulation* (Oxford University Press, Oxford ; New York, 2010).
- [59] Ceperley, D. M. Path integrals in the theory of condensed helium. *Reviews of Modern Physics* **67**, 279–355 (1995).
- [60] Heuer, A. & Büchner, S. Why is the density of inherent structures of a Lennard-Jones-type system Gaussian? *Journal of Physics: Condensed Matter* **12**, 6535–6541 (2000).
- [61] Neophytou, A. & Sciortino, F. Potential energy landscape of a coarse grained model for water: ML-BOP. *The Journal of Chemical Physics* **160**, 114502 (2024).
- [62] Sciortino, F., Kob, W. & Tartaglia, P. Inherent Structure Entropy of Supercooled Liquids. *Physical Review Letters* **83**, 3214–3217 (1999).
- [63] Sciortino, F., Kob, W. & Tartaglia, P. Thermodynamics of supercooled liquids in the inherent-structure formalism: A case study. *Journal of Physics: Condensed Matter* **12**, 6525–6534 (2000).
- [64] Allen, M. P. & Tildesley, D. J. *Computer Simulation of Liquids* Second edition edn (Oxford University Press, Oxford, United Kingdom, 2017).
- [65] Eltareb, A., Lopez, G. E. & Giovambattista, N. Nuclear quantum effects on the dynamics and glass behavior of a monatomic liquid with two liquid states. *The Journal of Chemical Physics* **156**, 204502 (2022).
- [66] Ceriotti, M. *et al.* Nuclear Quantum Effects in Water and Aqueous Systems: Experiment, Theory, and Current Challenges. *Chemical Reviews* **116**, 7529–7550 (2016).
- [67] Boerner, T. J., Deems, S., Furlani, T. R., Knuth, S. L. & Towns, J. *ACCESS: Advancing Innovation: NSF’s Advanced Cyberinfrastructure Coordination Ecosystem: Services & Support*, PEARC ’23, 173–176 (Association for Computing Machinery, New York, NY, USA, 2023).

A Appendix: Inherent Structure (E_{IS}) and Vibrational Energy (E_{vib}) for a Gaussian Potential Energy Landscape

Here, we show how the formal expressions for $E_{IS}(N, V, T)$ and $E_{vib}(N, V, T)$ are obtained in the PEL formalism. The PEL is assumed to be Gaussian. We consider

both cases where the harmonic approximation of the PEL holds (Eqs. 15 and 16), and where anharmonicities are included (Eqs. 18 and 20).

Harmonic PEL. The expression for E_{IS} (Eq. 15) follows from Eq. 8, using the expression for the configurational entropy of a Gaussian PEL (Eq. 10) and the vibrational Helmholtz free energy for a harmonic PEL (Eq. 11). Specifically, substituting Eqs. 10 and 11 into Eq. 8, one can show that,

$$1 - kT \left[- \left(\frac{e_{IS} - E_0}{\sigma^2} \right) \right] + kT \left(\frac{\partial \mathcal{S}}{\partial e_{IS}} \right)_{N,V,T} = 0 \quad \text{at } e_{IS} = E_{IS}. \quad (\text{A1})$$

It follows that,

$$E_{IS}(N, V, T) = E_0(V) - \sigma^2(V) (\beta + b(N, V, T, E_{IS})) \quad (\text{A2})$$

where $b(N, V, T, e_{IS}) \equiv \left(\frac{\partial \mathcal{S}(N, V, T, e_{IS})}{\partial e_{IS}} \right)_{N,V,T}$. Eq. A2 defines E_{IS} implicitly. However, for most systems studied, including the LJBM s studied in this work, it is found that $b = b(N, V, T)$ [see Eq. 30], and hence, Eq. A2 can be used to define E_{IS} explicitly. To do so, one first needs to calculate $\mathcal{S}(N, V, T, e_{IS})$, from which $b(N, V, T)$ is derived. Since the PEL variables E_0 and σ^2 are assumed to be T -independent (i.e., $E_0 = E_0(V)$ and $\sigma^2 = \sigma^2(V)$), these variables can be obtained by plotting $E_{IS}(T)$ as a function of $\beta + b$, and fitting the data using Eq. A2 [see, e.g., Fig. 4].

The expression for E_{vib} (Eq. 16) follows from the definition $E_{vib} \equiv E - E_{IS}$ and the thermodynamic expression $E = \left(\frac{\partial(\beta F)}{\partial \beta} \right)_{N,V}$. Since $F = -kT \ln Q$, it follows from Eq. 7 that,

$$E(N, V, T) = \left(\frac{\partial}{\partial \beta} \left[\beta E_{IS} - \frac{1}{k_B} S_{IS} + \beta F_{vib} \right] \right)_{N,V} \quad (\text{A3})$$

The first two terms of Eq. A3 can be calculated using Eq. 10 (Gaussian approximation),

$$\left(\frac{\partial}{\partial \beta} \left[\beta E_{IS} - \frac{1}{k_B} S_{IS} \right] \right)_{N,V} = \left(\frac{\partial}{\partial \beta} \left[\beta E_{IS} - \left(\alpha N - \frac{(E_{IS} - E_0)^2}{2\sigma^2} \right) \right] \right)_{N,V} \quad (\text{A4})$$

Using Eq. A2 in Eq. A4, one obtains the following expression,

$$\left(\frac{\partial}{\partial \beta} \left[\beta E_{IS} - \frac{1}{k_B} S_{IS} \right] \right)_{N,V} = E_{IS} - N \left(\frac{\partial \alpha}{\partial \beta} \right)_V + \beta \left(\frac{E_0}{\partial \beta} \right)_V + \frac{1}{2} \left(\frac{\partial \sigma^2}{\partial \beta} \right)_V (\beta^2 + b^2) + b\sigma^2 \left[1 + \left(\frac{\partial b}{\partial \beta} \right)_{N,V} \right] \quad (\text{A5})$$

The last term of Eq. A3 can be calculated using Eq. 11 (harmonic approximation),

$$\left(\frac{\partial(\beta F_{vib})}{\partial \beta} \right)_{N,V} = 3Nn_b k_B T + \left[\frac{\partial \mathcal{S}(N, V, T, E_{IS})}{\partial \beta} \right]_{N,V} \quad (\text{A6})$$

Since $\mathcal{S} = \mathcal{S}(N, V, T, E_{IS})$, it follows that

$$\begin{aligned} \left(\frac{\partial \mathcal{S}}{\partial \beta}\right)_{N,V} &= \left(\frac{\partial \mathcal{S}}{\partial \beta}\right)_{N,V,E_{IS}} + \left(\frac{\partial \mathcal{S}}{\partial E_{IS}}\right)_{N,V,\beta} \left(\frac{\partial E_{IS}}{\partial \beta}\right)_{N,V} \\ &= \left(\frac{\partial \mathcal{S}}{\partial \beta}\right)_{N,V,E_{IS}} + b \left(\frac{\partial E_{IS}}{\partial \beta}\right)_{N,V} \end{aligned} \quad (\text{A7})$$

Using Eq. A2 in Eq. A7, and then replacing the result into Eq. A5, one finds that

$$\left(\frac{\partial(\beta F_{vib})}{\partial \beta}\right)_{N,V} = 3Nn_b k_B T + \left(\frac{\partial \mathcal{S}}{\partial \beta}\right)_{N,V,E_{IS}} + b \left[\left(\frac{\partial E_0}{\partial \beta}\right)_V - \sigma^2 \left(\frac{\partial}{\partial \beta}(\beta + b)\right)_V - \left(\frac{\partial \sigma^2}{\partial \beta}\right)_V (\beta + b) \right] \quad (\text{A8})$$

Using Eqs. A5 and A8 in Eq. A3, the following expression for the energy follows,

$$E(N, V, T) = E_{IS} + \left\{ 3Nn_b k_B T + \left(\frac{\partial \mathcal{S}}{\partial \beta}\right)_{N,V,E_{IS}} \right. \quad (\text{A9})$$

$$\left. - N \left(\frac{\partial \alpha}{\partial \beta}\right)_V + (b + \beta) \left(\frac{\partial E_0}{\partial \beta}\right)_V - \frac{1}{2}(b + \beta)^2 \left(\frac{\partial \sigma^2}{\partial \beta}\right)_V \right\} \quad (\text{A10})$$

where the curly bracket is $E_{vib} \equiv E - E_{IS}$. For the case where E_0 , σ^2 , and α are T -independent, one finds that

$$E_{vib}(N, V, T) = 3Nn_b k_B T + \left(\frac{\partial \mathcal{S}(N, V, T, E_{IS})}{\partial \beta}\right)_{N,V,E_{IS}} \quad (\text{A11})$$

Anharmonic PEL. To obtain the expressions for E_{IS} and E_{vib} , for a Gaussian and anharmonic PEL, we follow the same procedure outlined above. To do so, we first note that, in the presence of anharmonicities, the vibrational Helmholtz free energy is given by Eq. 17, which we rewrite as follows,

$$F_{vib}(N, V, T, e_{IS}) \approx 3Nn_b k_B T \ln(\beta \hbar \omega_0) + k_B T [\mathcal{S}(N, V, T, e_{IS}) + \beta F_{vib}^{anh}(N, V, T)] \quad (\text{A12})$$

The square bracket can be interpreted as an *effective* shape function,

$$\mathcal{S}_{eff}(N, V, T, e_{IS}) \equiv \mathcal{S}(N, V, T, e_{IS}) + \beta F_{vib}^{anh} \quad (\text{A13})$$

that takes into account the corrections due to the anharmonicities in the PEL basins, about the corresponding IS. This means that the vibrational Helmholtz free energy is given by Eq. 11, substituting $\mathcal{S}_{eff}(N, V, T, e_{IS})$ for $\mathcal{S}(N, V, T, e_{IS})$,

$$F_{vib}(N, V, T) = 3Nn_b k_B T \ln(\beta \hbar \omega_0) + k_B T \mathcal{S}_{eff}(N, V, T, e_{IS}) \quad (\text{A14})$$

Using Eq. A14, we can obtain E_{IS} and E_{vib} .

The expression for E_{IS} (Eq. 18) follows from Eq. 8, with the configurational entropy given by Eq. 10 (Gaussian approximation), and the vibrational Helmholtz free energy

given by Eq. A14. Substituting Eqs. 10 and A14 into Eq. 6, one can show that,

$$1 - kT \left[-\frac{(e_{IS} - E_0)}{\sigma^2} \right] + kT \left(\frac{\partial \mathcal{S}_{eff}}{\partial e_{IS}} \right)_{N,V,T} = 0 \quad \text{at} \quad e_{IS} = E_{IS} \quad (\text{A15})$$

Using Eq. A13 in Eq. A15, it follows that,

$$E_{IS}(N, V, T) = E_0 - \sigma^2 (b + \beta) - \sigma^2 \left(\frac{\partial \beta F_{vib}^{anh}}{\partial e_{IS}} \right)_{N,V,T,e_{IS}=E_{IS}} \quad (\text{A16})$$

which is identical to Eq. 18.

The expression for E_{vib} (Eq. 20) follows from the definition $E_{vib} \equiv E - E_{IS}$ and the thermodynamic expression $E = \left(\frac{\partial(\beta F)}{\partial \beta} \right)_{N,V}$. Since $F = -kT \ln Q$, it follows from Eq. 7 that the total energy is given by Eq. A3 even if anharmonicities are included. In the presence of anharmonicities, however, one must replace $\mathcal{S}(N, V, T, e_{IS})$ with $\mathcal{S}_{eff}(N, V, T, e_{IS})$ in the definition of F_{vib} [see Eqs. 11 and A14]. The same mathematical steps followed in the case of harmonic PELs [Eqs. A3–A11] can then be applied for anharmonic PELs. This implies that, in the presence of anharmonicities, Eq. A11 holds after substituting $\mathcal{S}_{eff}(N, V, T, e_{IS})$ for $\mathcal{S}(N, V, T, e_{IS})$. Therefore,

$$E_{vib} = 3Nn_b kT + \left(\frac{\partial \mathcal{S}_{eff}(N, V, T, E_{IS})}{\partial \beta} \right)_{N,V,E_{IS}} \quad (\text{A17})$$

Using Eq. A13 in Eq. A17, one obtains the expression for E_{vib} ,

$$E_{vib}(N, V, T) = 3Nn_b kT + \left(\frac{\partial \mathcal{S}(N, V, T)}{\partial \beta} \right)_{N,V,E_{IS}} + \left(\frac{\partial(\beta F_{vib}^{anh}(N, V, T))}{\partial \beta} \right)_{N,V,E_{IS}} \quad (\text{A18})$$

which is identical to Eq. 20.

B Appendix: Relationship between the Temperature-dependence of the PEL of a quantum liquid and the *springs* potential energy of the corresponding ring-polymer system

Here we show that, within the harmonic approximation of the PEL, the potential energy of the ring-polymer's springs,

$$E_{sp}(N, V, T) \equiv \left\langle \sum_{i=1}^N \sum_{k=1}^{n_b} \frac{1}{2} k_i^{sp} (\mathbf{r}_i^{k+1} - \mathbf{r}_i^k)^2 \right\rangle_{N,V,T}$$

controls the temperature dependence of the PEL. Specifically, we show that

$$\left(\frac{\partial \mathcal{S}(N, V, T, e_{IS})}{\partial \beta} \right)_{N, V, e_{IS}=E_{IS}} = 2 E_{sp}(N, V, T) \quad (\text{B1})$$

To do so, we introduce an imaginary ring-polymer (IRP) system as follows. At a given temperature T , the ring-polymer system associated to the quantum liquid (briefly, “the” RP system) is characterized by a spring constant $k^{sp}(T) = mn_b/(\beta\hbar)^2$. We define the IRP system so its spring constant k_0 is T -independent and given by $k_0 \equiv k_{sp}(T)$. Hence, while the PEL of the RP system (associated to the quantum liquid) varies with T , the PEL of the IRP does not. The IRP system is a truly classical system in the sense that its PEL, and hence its Hamiltonian, do not vary with T . Importantly, at the original temperature T , and only at this T , both IRP and the original RP share the same PEL, including the inherent structures available in the PEL.

Now, consider the evolution of the IRP (with constant spring constant k_0) and the RP associated to the quantum liquid [with spring constant $k^{sp}(T)$] upon heating/cooling. The total energy of the original RP system is given by Eq.14 and 16 (harmonic approximation),

$$E(N, V, T) = E_{IS}(N, V, T) + 3N n_b k T + \left(\frac{\partial \mathcal{S}(N, V, T, e_{IS})}{\partial \beta} \right)_{N, V, e_{IS}=E_{IS}} \quad (\text{B2})$$

Instead, for the IRP (T -independent PEL), the total energy (harmonic approximation) is given by

$$E^{IRP} = E_{IS}(N, V, T) + 3N n_b k T \quad (\text{B3})$$

As shown in Ref. [58],

$$E(N, V, T) = E^{IRP} - 2 E^{sp}.$$

Therefore, by substituting Eqs. B2 and B3 into this expression, one obtains Eq. B1.